LA-UR-23-27164

Approved for public release; distribution is unlimited.

Title:	Elucidating the chiral anomaly in the electronic structure of Dirac materials
Author(s):	Peterson, Elizabeth Ann Lane, Christopher A. Zhu, Jianxin
Intended for:	International Conference on Strongly Correlated Electron Systems 2023, 2023-07-02/2023-07-07 (Incheon, Korea, South)
Issued:	2023-07-03

Los Alamos NATIONAL LABORATORY

Elucidating the chiral anomaly in the electronic structure of Dirac materials

Elizabeth A. Peterson
Los Alamos National Laboratory - Theoretical Division (T-4)

International Conference on Strongly Correlated Electron Systems 2023
Incheon, South Korea
05 July 2023

Quantum Anomalies

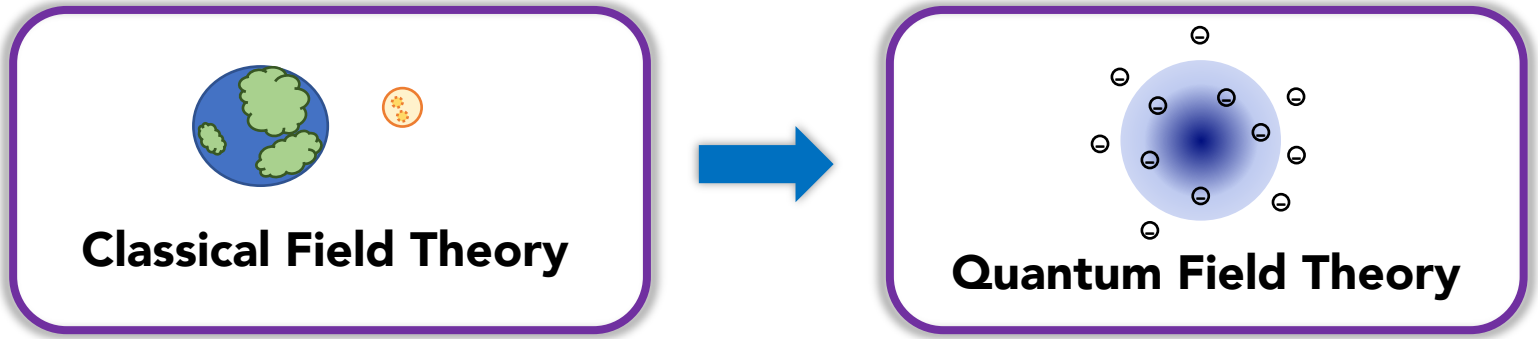

Implication of Noether's theorem:
The symmetry-breaking process from classical field theory to quantum field theory results in a "quantum anomaly" and each known quantum anomaly leads to a different non-conserved current which *must* be measurable

Experimental tests of quantum theory in General Relativity generally intractable

Condensed matter offers experimental cradle to explore physics of Universe

Chiral anomaly in DSMs

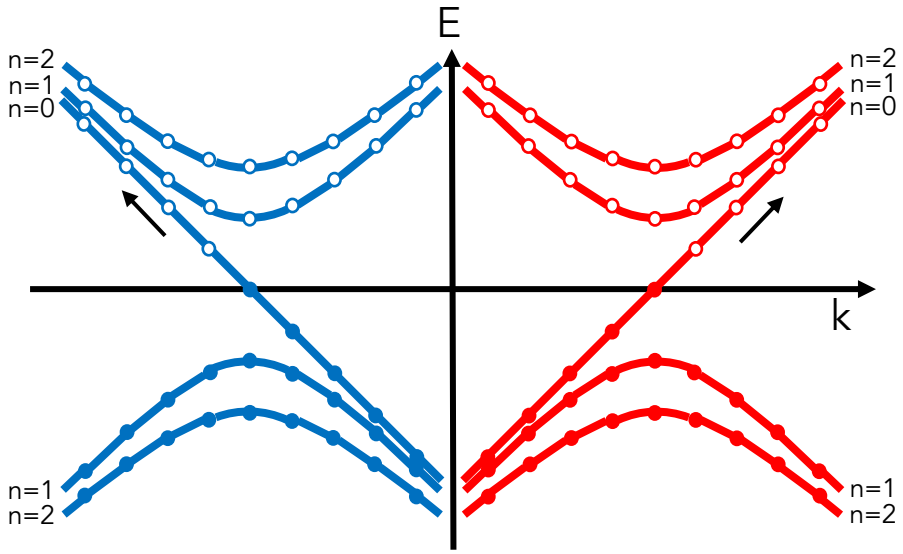

Energy spectrum in magnetic field split into Landau levels

Left- and right-handed chiral fermions expected to have equal populations

Chiral anomaly in DSMs

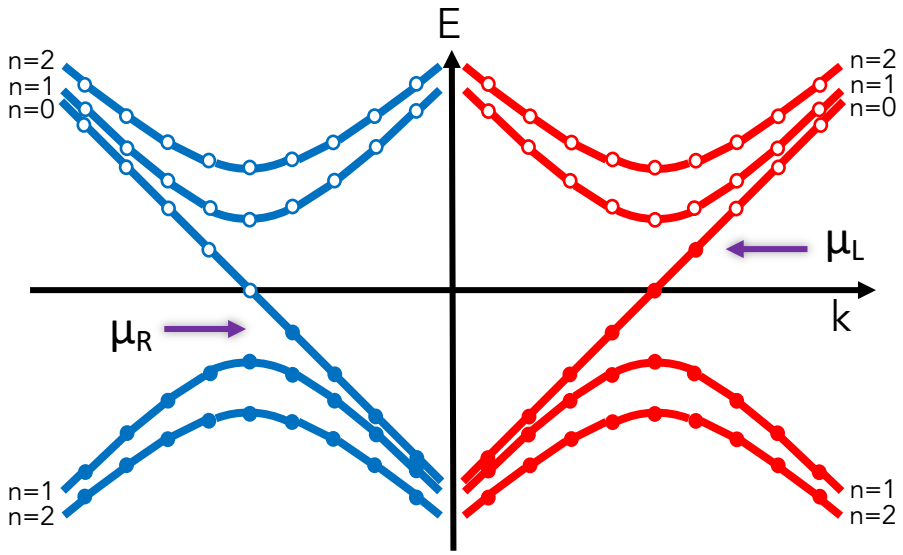

Energy spectrum in magnetic field split into Landau levels

Left- and right-handed chiral fermions expected to have equal populations

But in some cases they don't!
→ **Chiral anomaly**

Experimental Signature of Chiral Anomaly

chiral chemical potential $\mu_5 \equiv \frac{\mu_R - \mu_L}{2}$

No external fields

$\mu_5 = \mu_L = \mu_R = 0$

External fields

chiral charge density

$\rho_5 \sim \boldsymbol{E} \cdot \boldsymbol{B}$

Parallel electric and magnetic fields
→ **chiral magnetic effect (CME)**

$\sigma_{CME} \sim B^2$

Negative longitudinal magnetoresistance (NLMR)

$J = J_{Ohm} + J_{CME} = (\sigma_{Ohm} + \sigma_{CME})E$

Q. Li, et al., *Nat. Phys.*, **12**, 550 (2016)

Anomalous transport properties in $ZrTe_5$ and $HfTe_5$

Labels

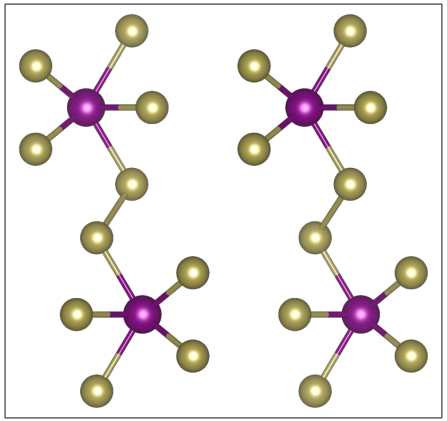

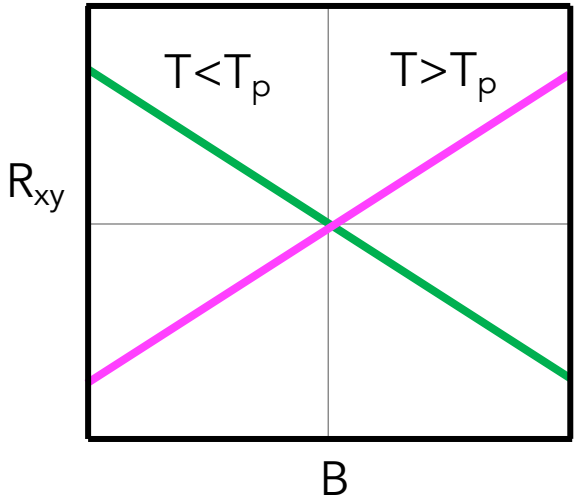

- Negative longitudinal magnetoresistance
- Sign of charge carriers changes at critical temperature (Lifshiftz transition)

Y. Zhang, et al., *Nat. Commun.*, **8**, 15512 (2017)
H. Chi, et al., *New J. Phys.*, **19**, 015005 (2017)
P. Shahi, et al., *Phys Rev X*, **8** 021055 (2018)
S. Galeski, et al., *Nat. Commun.* **11**, 5926 (2020)
Q. Xie, et al., *Appl. Phys. Lett.*, **120**, 141903 (2022)

Fermi energy shift with varying temperature

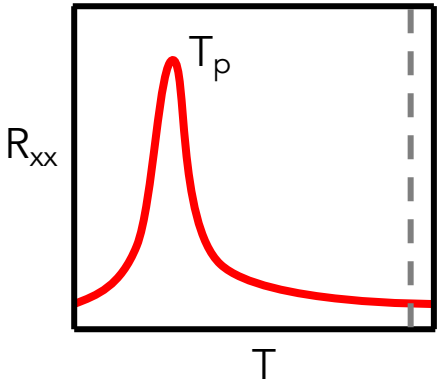

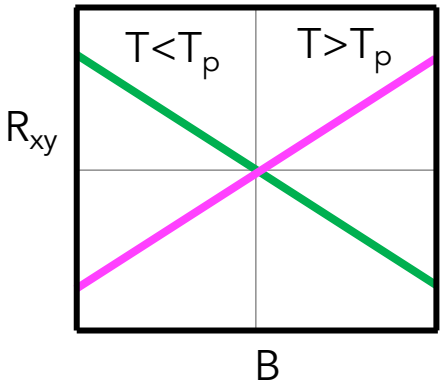

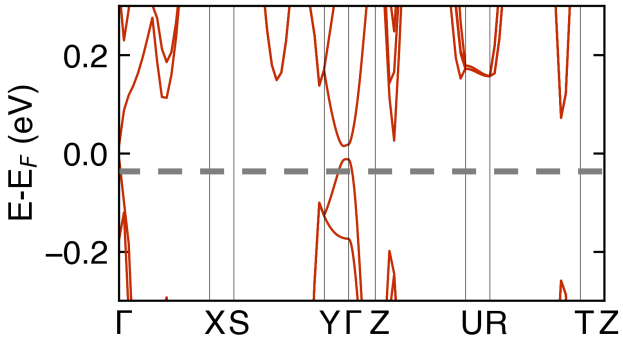

Lifshitz transition characterized by shifting of Fermi energy with changing temperature

ARPES

Y. Zhang, et al., *Nat. Commun.*, **8**, 15512 (2017)

Fermi energy shift with varying temperature

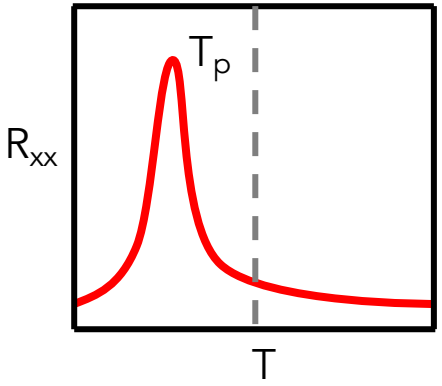

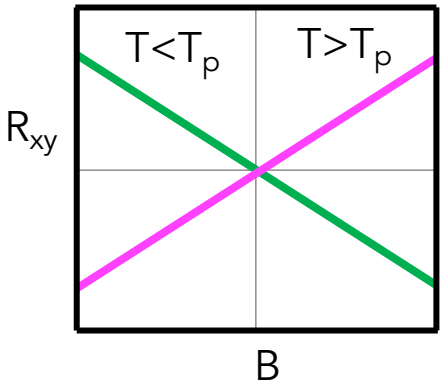

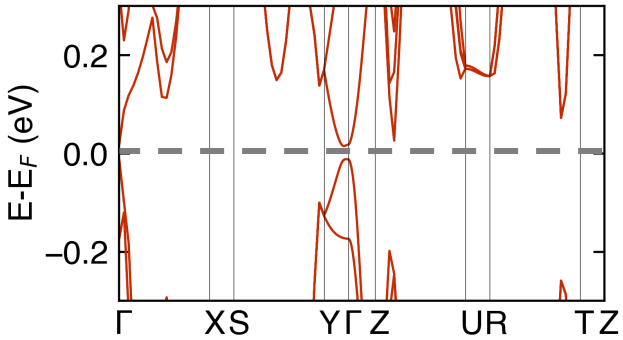

Lifshitz transition characterized by shifting of Fermi energy with changing temperature

ARPES

Y. Zhang, et al., *Nat. Commun.*, **8**, 15512 (2017)

Fermi energy shift with varying temperature

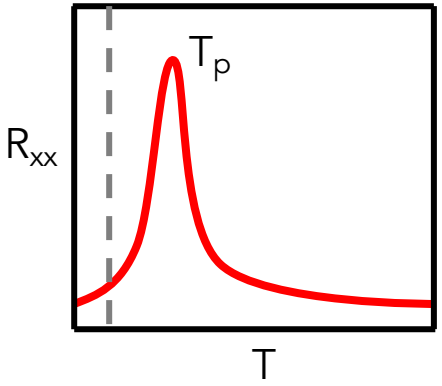

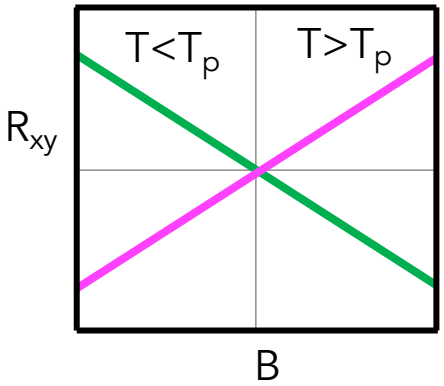

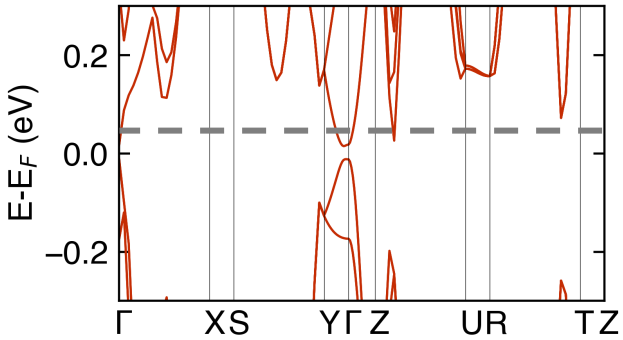

Lifshitz transition characterized by shifting of Fermi energy with changing temperature

ARPES

Y. Zhang, et al., *Nat. Commun.*, **8**, 15512 (2017)

Probe anomalous transport via electronic structure

Te Vacancies

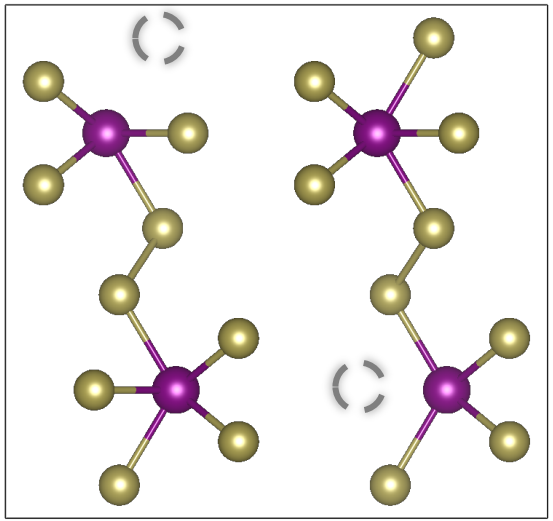

Applied B Field

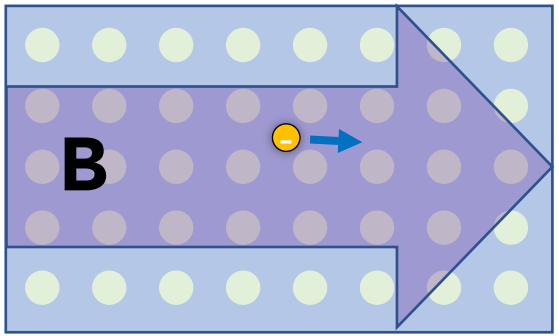

Probe anomalous transport via electronic structure

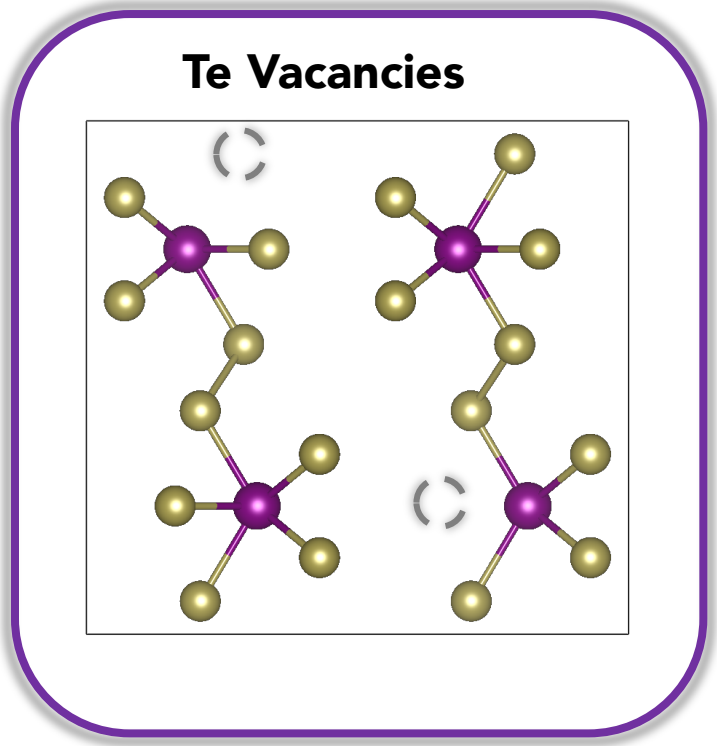

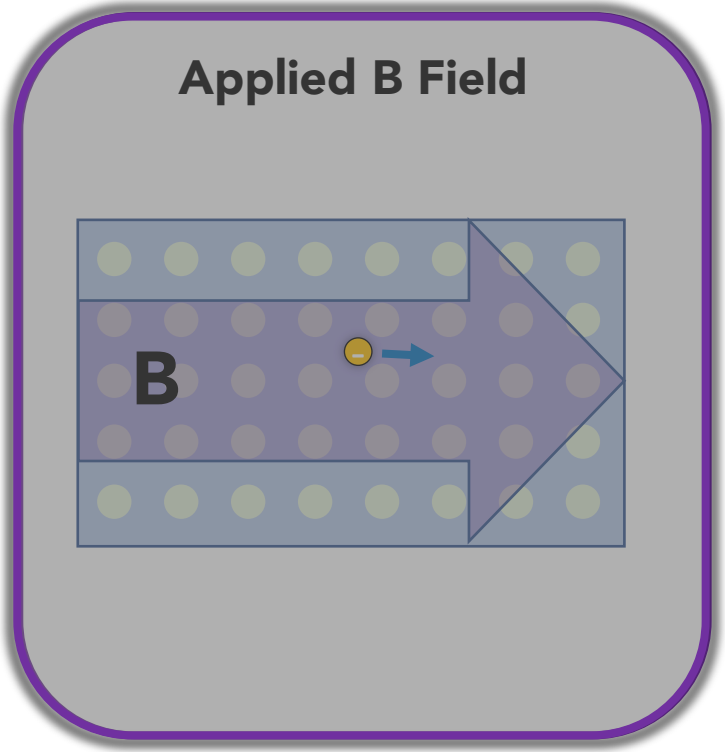

Electronic structure tuning knobs

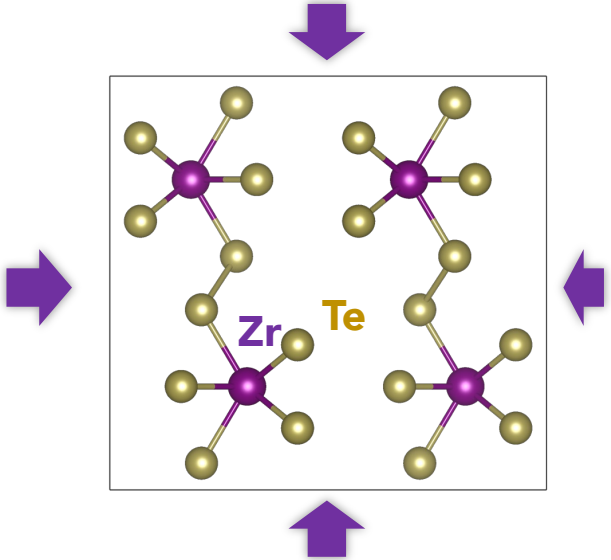

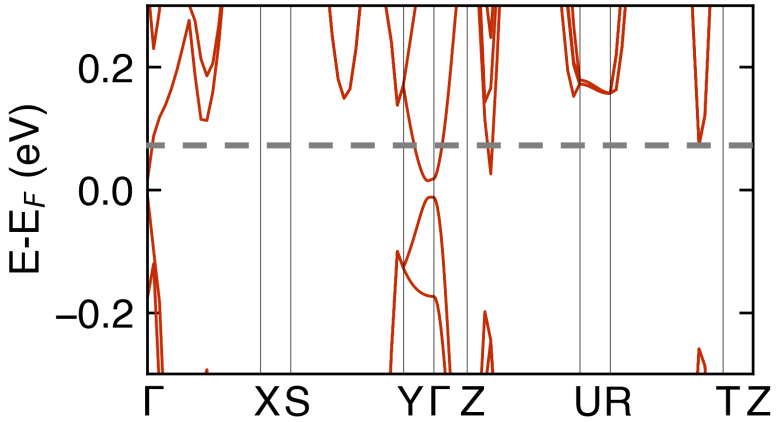

Volume / Lattice Parameters

Chemical potential

Te vacancies drive anomalous transport behavior

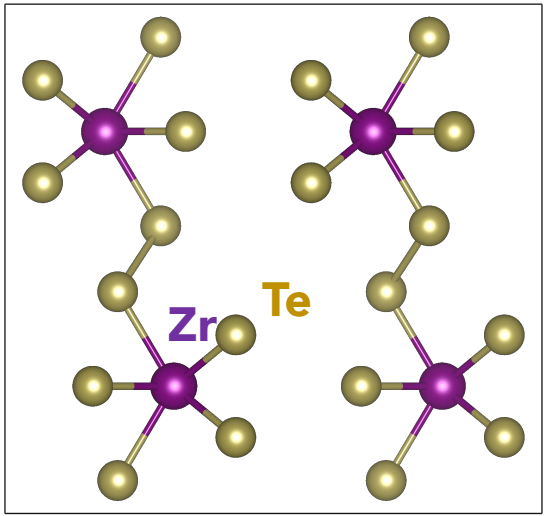

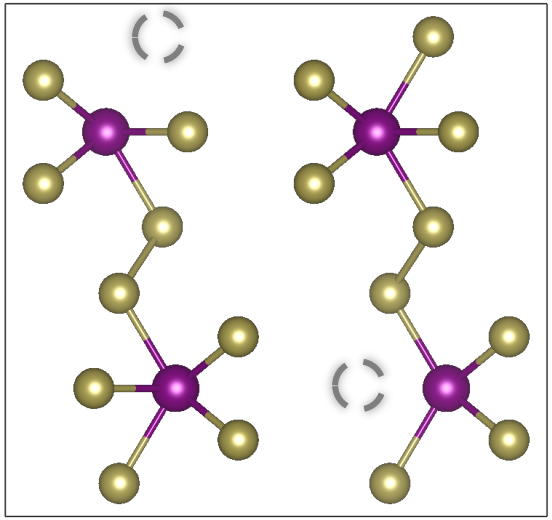

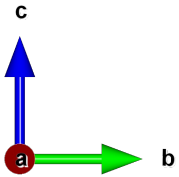

$ZrTe_5$ grown with higher density of Te vacancies exhibits stronger NLMR

Q. Li, et al., *Nat. Phys.*, **12**, 550 (2016)
P. Shahi, et al., *Phys Rev X*, **8** 021055 (2018)

→ Method for tuning both **volume** and **chemical potential**

What might Te vacancies be doing?

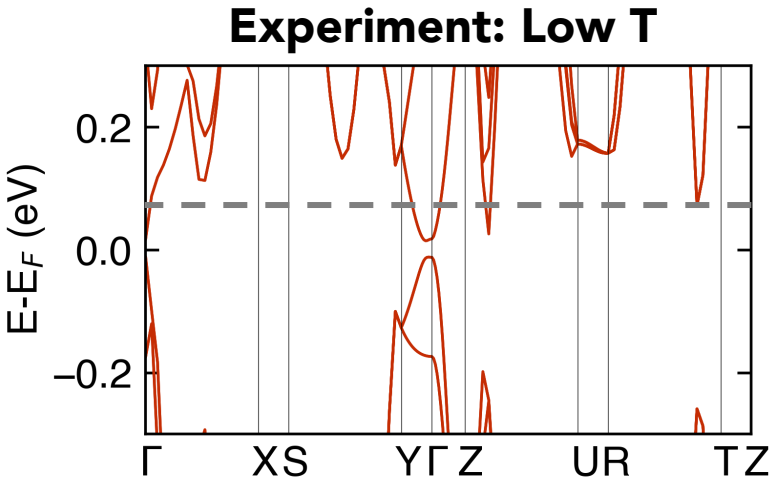

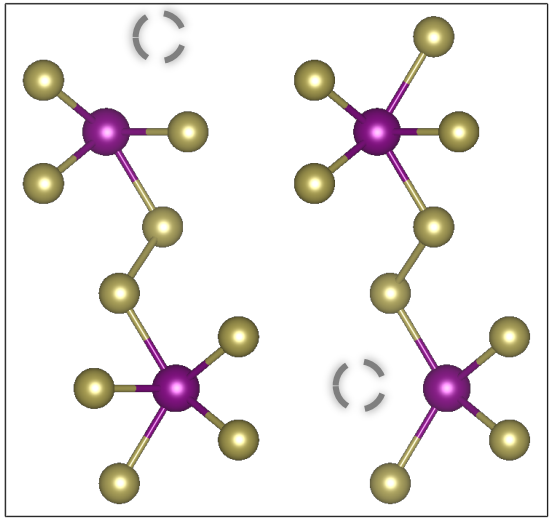

Intuition

Anion vacancies promote n-type conduction (excess electron carriers)

Investigation of Te vacancies in $ZrTe_5$ and $HfTe_5$

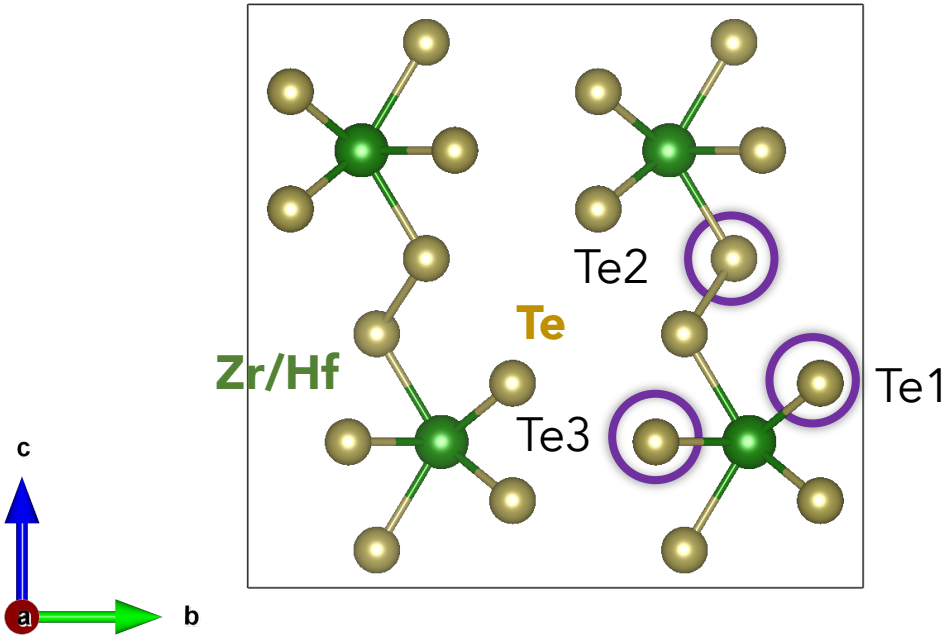

Multiple symmetrically distinct Te vacancy sites

Experiment suggests Te vacancies can proliferate up to 3-4% in $ZrTe_5$

P. Shahi, et al., *Phys Rev X*, **8** 021055 (2018)

Investigation of Te vacancies in $ZrTe_5$ and $HfTe_5$

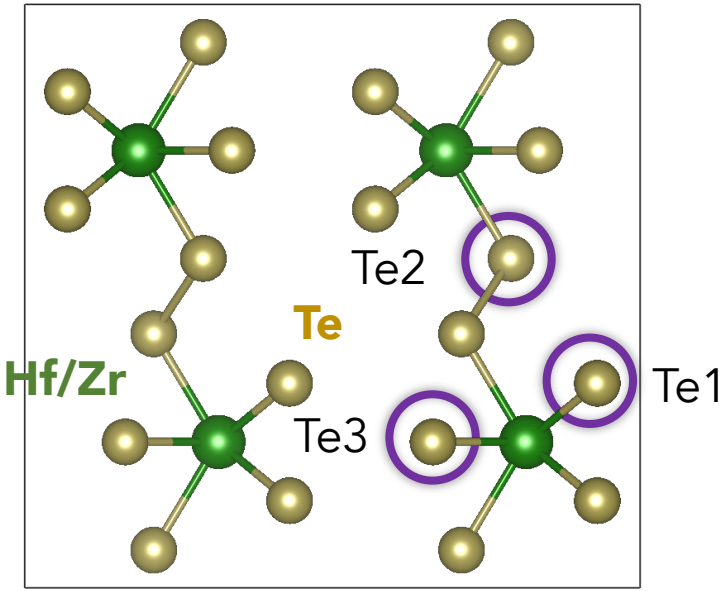

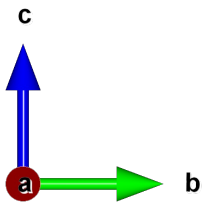

Te vacancies (~2%)
Defect formation energy (meV/atom)

	Te1	Te2	Te3
$ZrTe_5$	83.1	88.2	97.6
$HfTe_5$	77.0	83.5	94.8

Calculation details

VASP
PBE+D3
2x1x1 supercell

ENCUT 500 eV
kgrid 10x8x8
Forces < 0.001 eV/Å

Peterson, Lane, Zhu, *in preparation*

$ZrTe_5$ band structure with Te vacancies

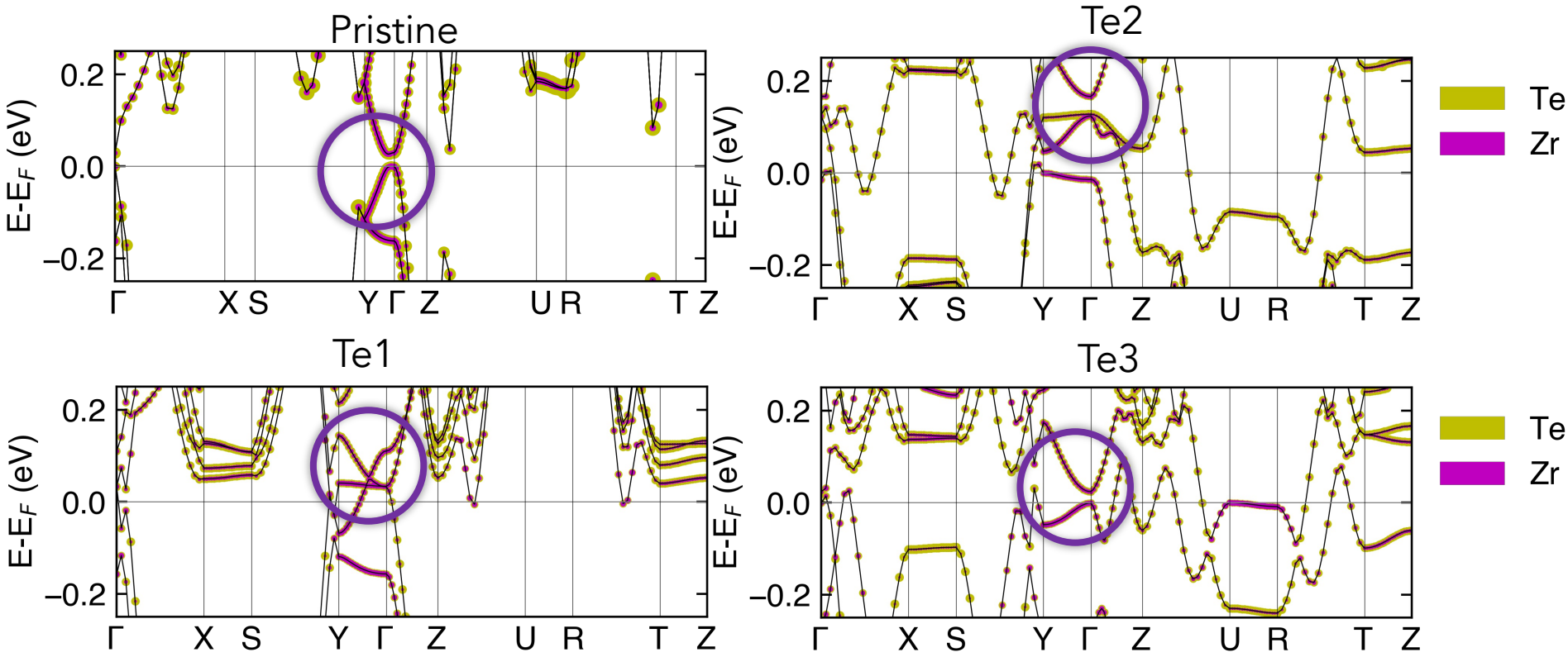

Te vacancies shift **chemical potential** to **lower** energy

Peterson, Lane, Zhu, *in preparation*

Probe anomalous transport via electronic structure

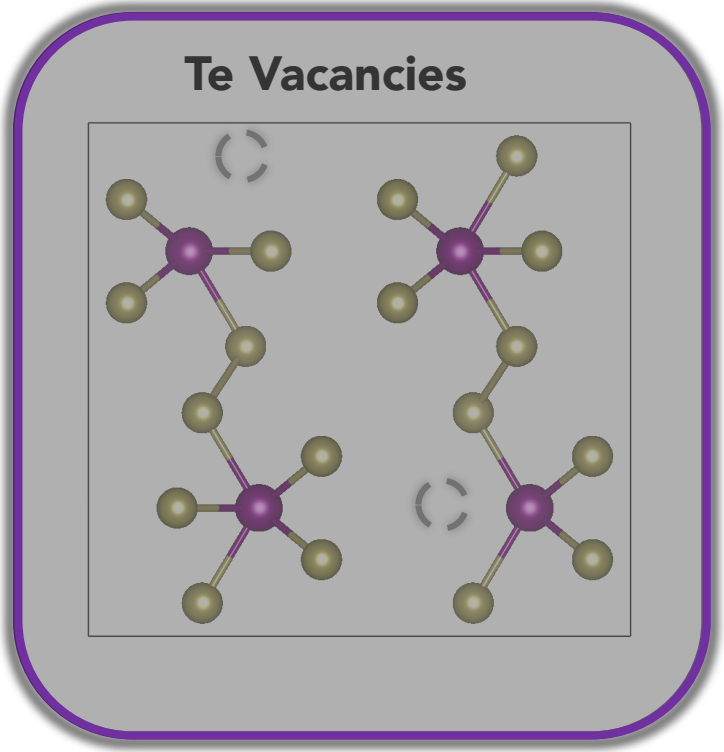

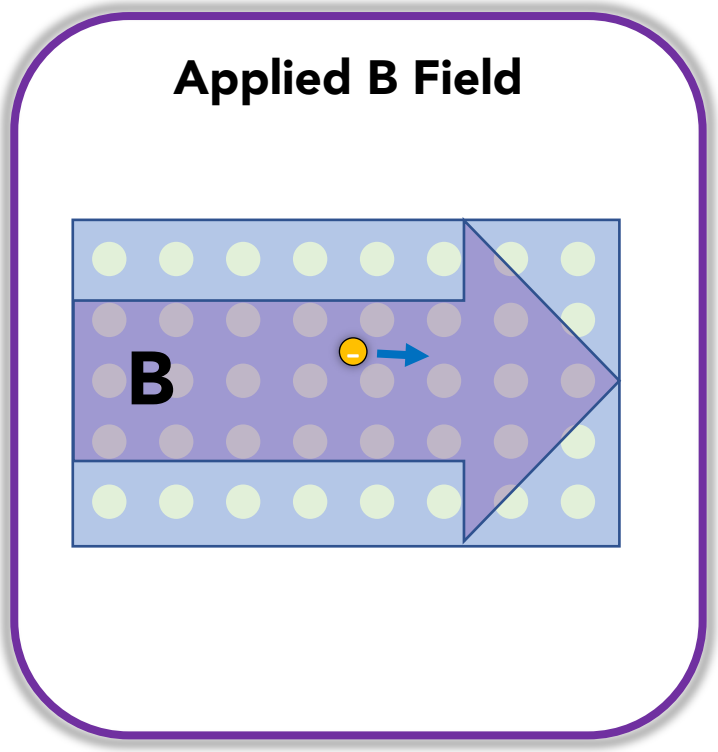

Electrons interacting with static magnetic fields

Electrons in a Static Magnetic Field (Semiclassical)

$$H = \frac{1}{2m}\sum_i \left(\boldsymbol{p}_i + \frac{e}{c}\boldsymbol{A}(\boldsymbol{r}_i)\right)^2 + V(\boldsymbol{r}_i)$$

Zeeman contribution

$$H_Z \sim \boldsymbol{S_i} \cdot \boldsymbol{B}$$

Really small
B = 1T → ~50 μeV

Orbital contribution

Peierl's substitution

$$h_{ij}(\boldsymbol{r}) = -t_{i\neq j}e^{i\varphi_{ij}} + (\epsilon_i - E_F)\delta_{ij}$$

$$\varphi_{ij} = -\frac{e}{\hbar c}\int_{\boldsymbol{R}_j}^{\boldsymbol{R}_i} \boldsymbol{A}(\boldsymbol{\xi}) \cdot \boldsymbol{\xi}$$

Modeling effects of applied magnetic field

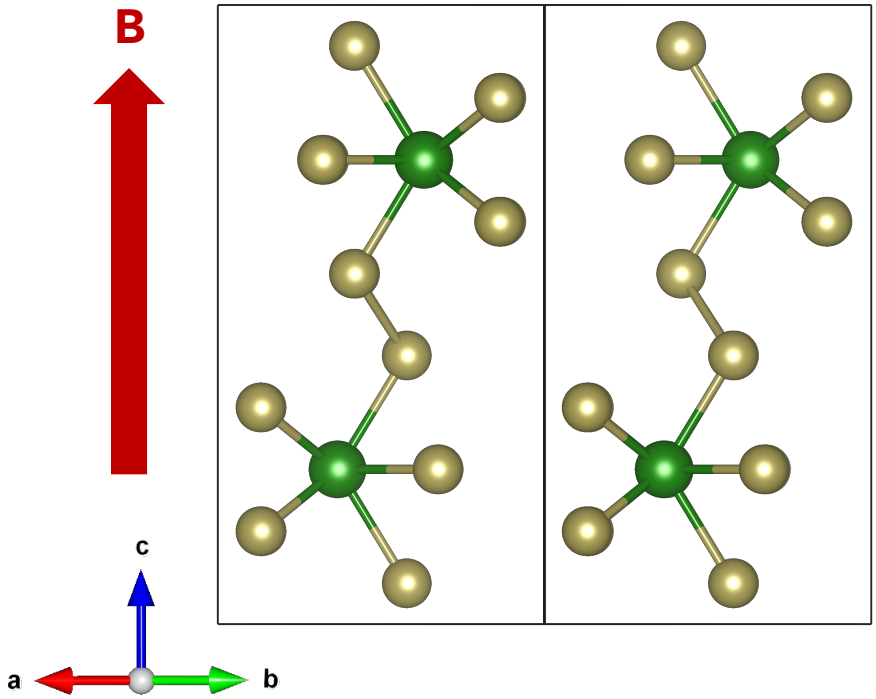

Probe effect of **applied magnetic field** on **electronic structure** by building Model Hamiltonian from Wannierized DFT band structure

$$H = \sum_{ij} \widetilde{t_{ij}} c_i^+ c_j + g\mu_B \boldsymbol{\sigma} \cdot \boldsymbol{B}$$

Calculation details

DFT	**Wannierization**
WIEN2K	Wannier90 (Hf: d, Te: p orbitals)

Modeling effects of *experimental* magnetic field

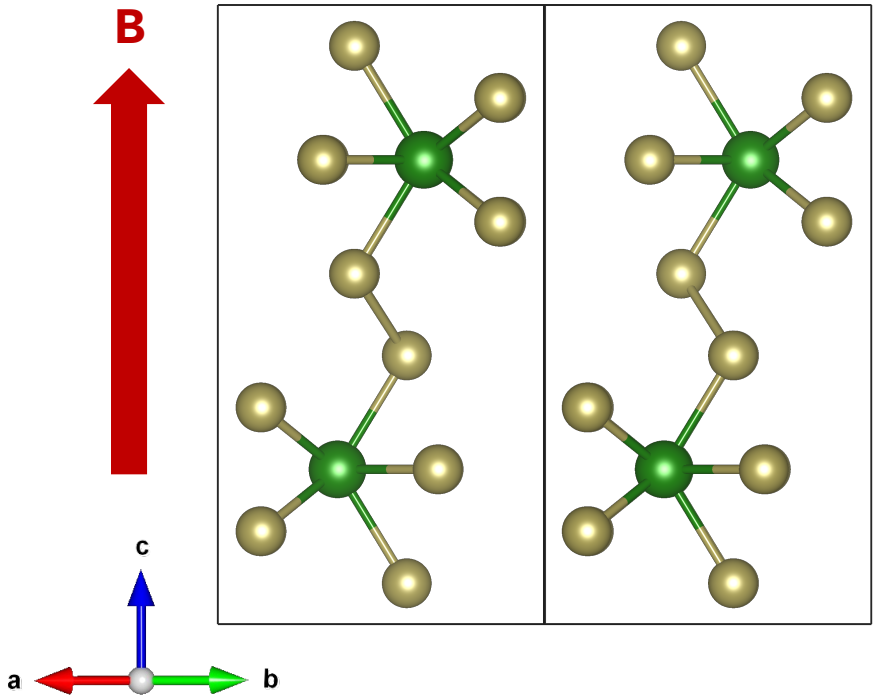

Orbital contribution

$$h_{ij}(\boldsymbol{r}) = -t_{i\neq j}e^{i\varphi_{ij}} + (\epsilon_i - E_F)\delta_{ij}$$

$$\varphi_{ij} = -\frac{e}{\hbar c}\int_{\boldsymbol{R}_j}^{\boldsymbol{R}_i} \boldsymbol{A}(\boldsymbol{\xi})\cdot\boldsymbol{\xi}$$

In general

Vector potential ($\mathrm{A}(\mathrm{r})$) changes periodicity of lattice → supercell

In experimental regime

Applied fields ~10^{-4} Φ_0 → perturbative expansion in $\mathrm{A}(\mathrm{r})$

Band structure without applied magnetic field

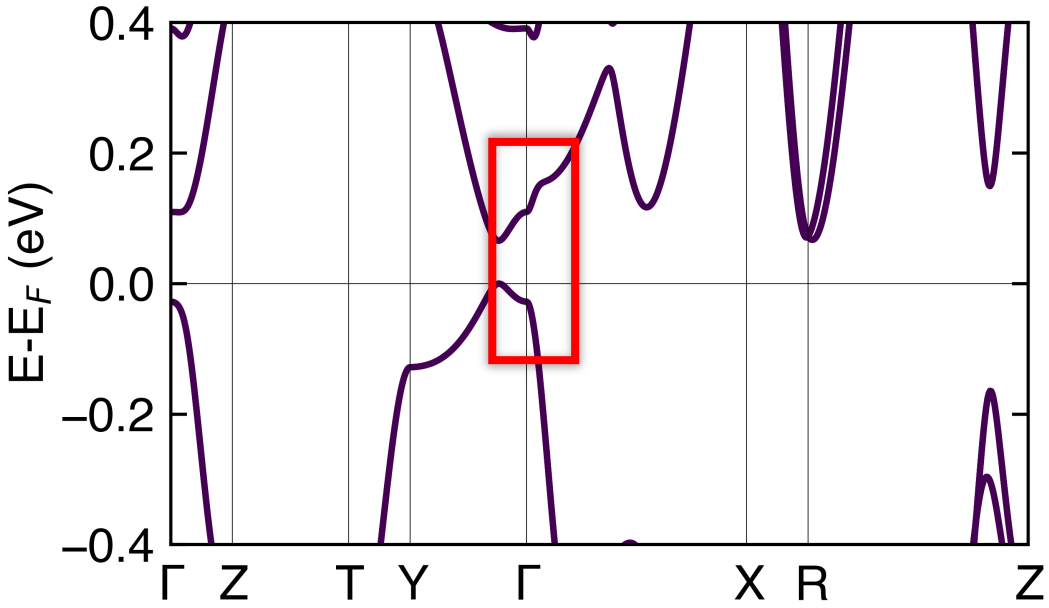

Investigate effect of applied magnetic field at Brillouin zone center (**Γ**)

Peterson, Lane, Zhu, *in preparation*

Effects of experimentally probed magnetic fields

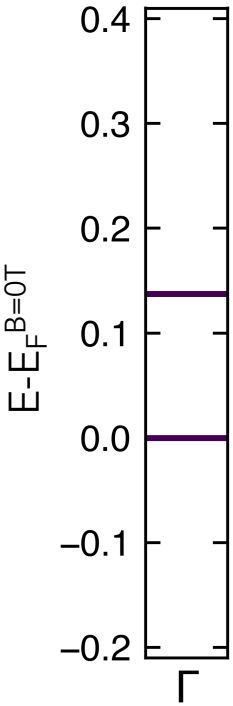

Peterson, Lane, Zhu, *in preparation*

Effects of experimentally probed magnetic fields

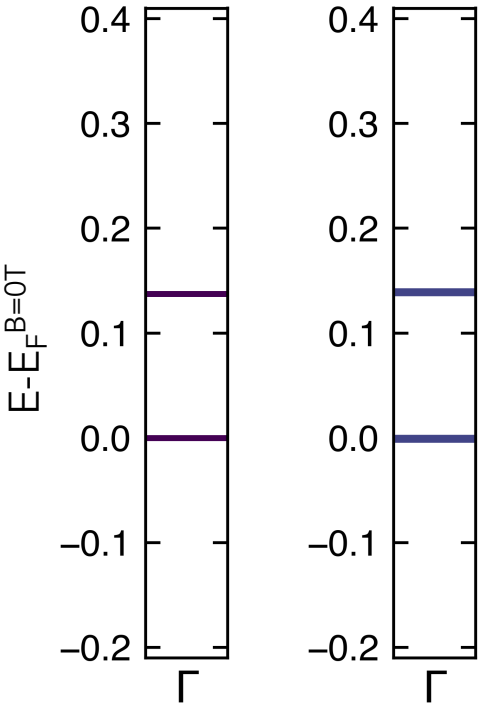

Peterson, Lane, Zhu, *in preparation*

Effects of experimentally probed magnetic fields

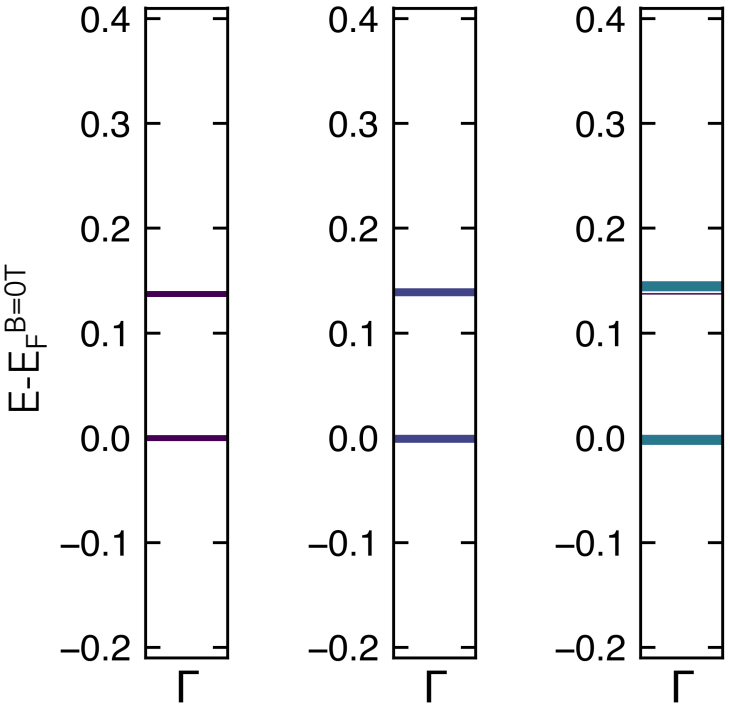

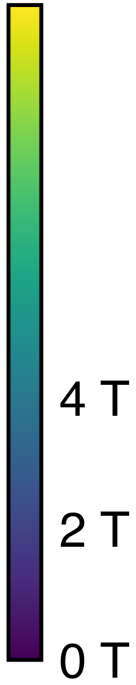

Peterson, Lane, Zhu, *in preparation*

Effects of experimentally probed magnetic fields

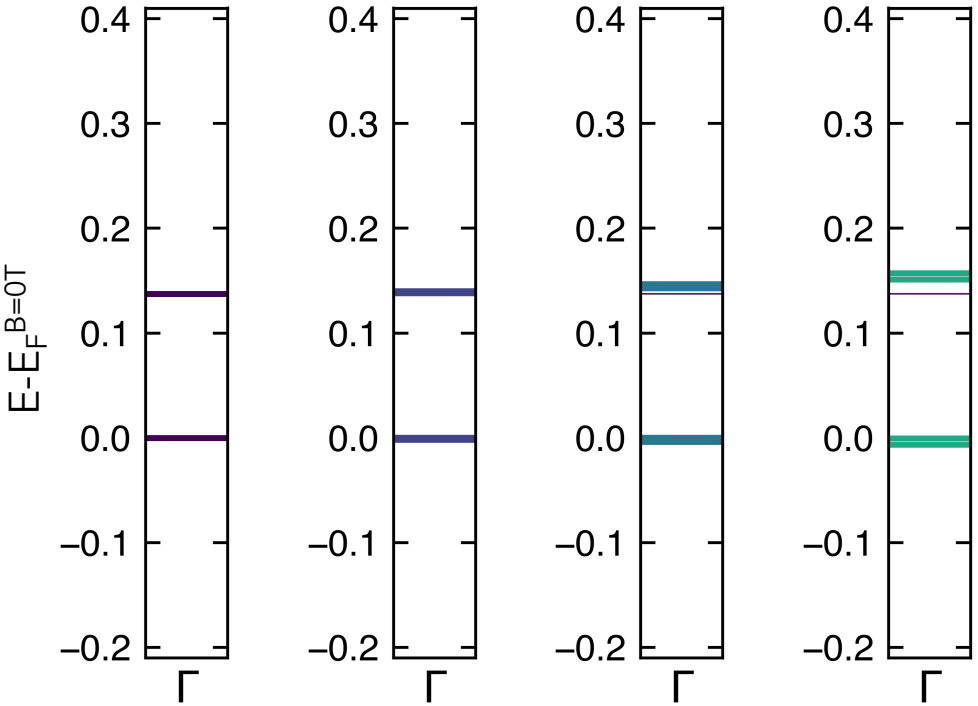

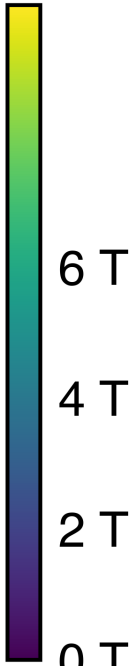

Peterson, Lane, Zhu, *in preparation*

Effects of experimentally probed magnetic fields

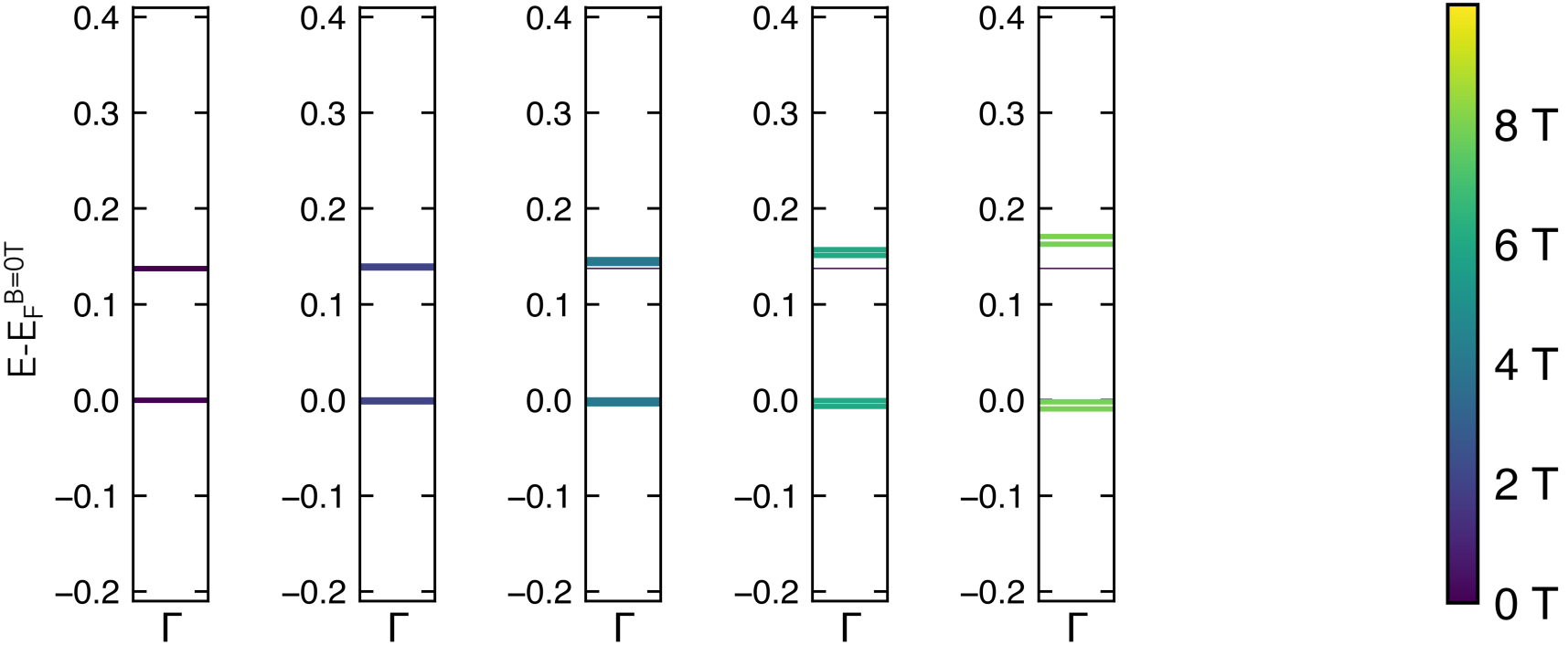

Peterson, Lane, Zhu, *in preparation*

Effects of experimentally probed magnetic fields

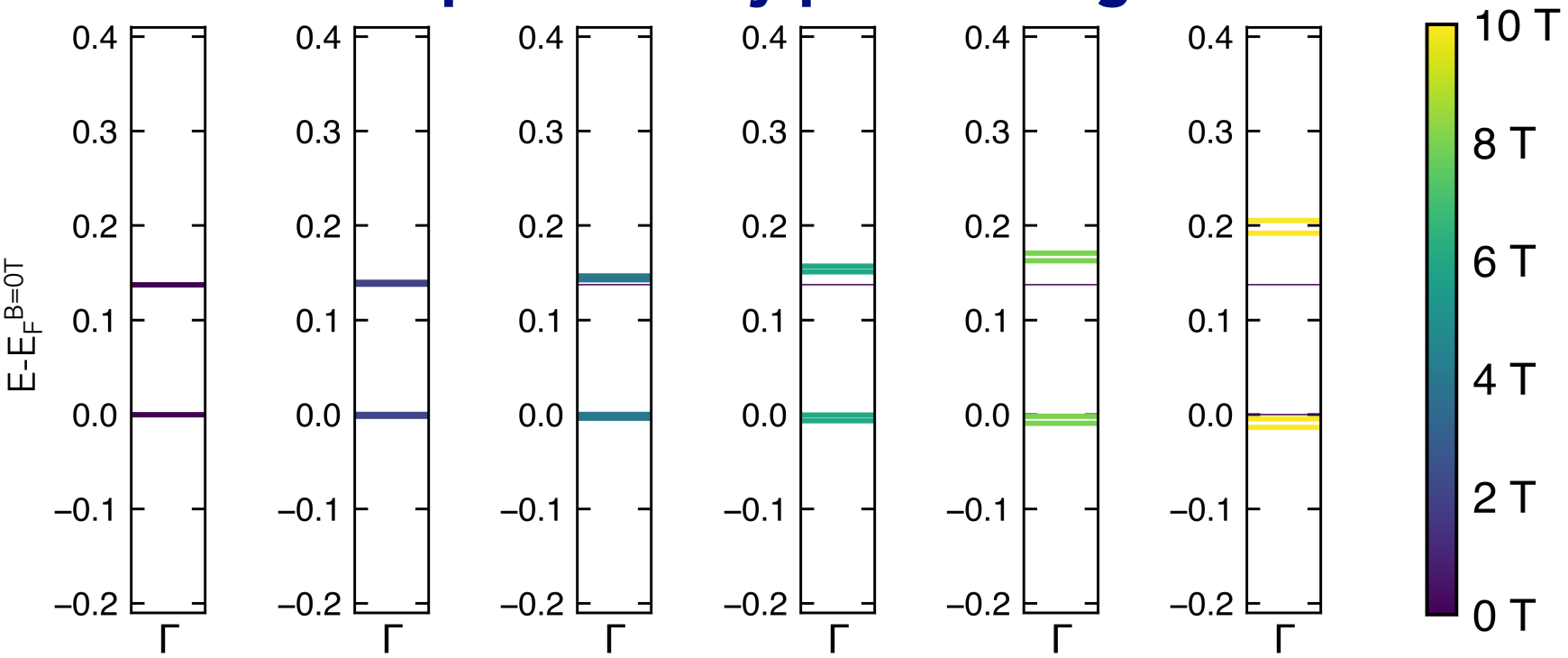

Applied magnetic field along chain direction

increases band gap and shifts **chemical potential** to **higher** energy

Peterson, Lane, Zhu, *in preparation*

Effects of experimentally high magnetic fields

Peterson, Lane, Zhu, *in preparation*

Effects of experimentally high magnetic fields

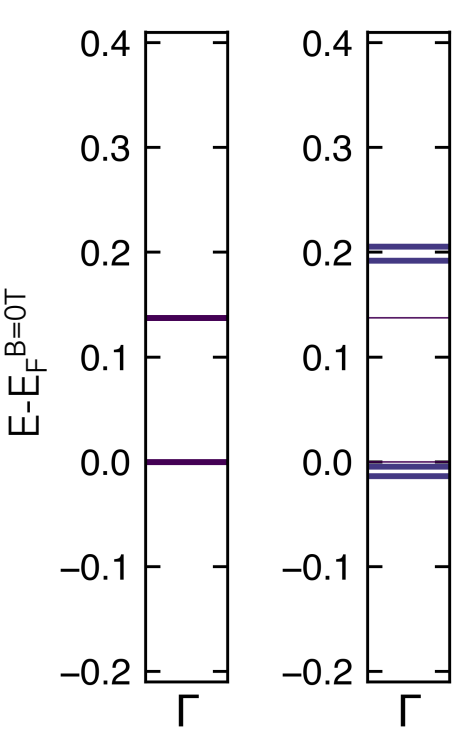

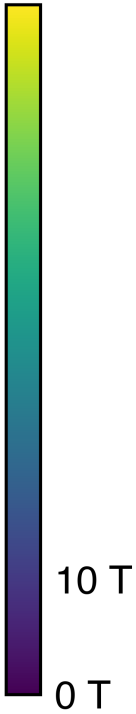

Peterson, Lane, Zhu, *in preparation*

Effects of experimentally high magnetic fields

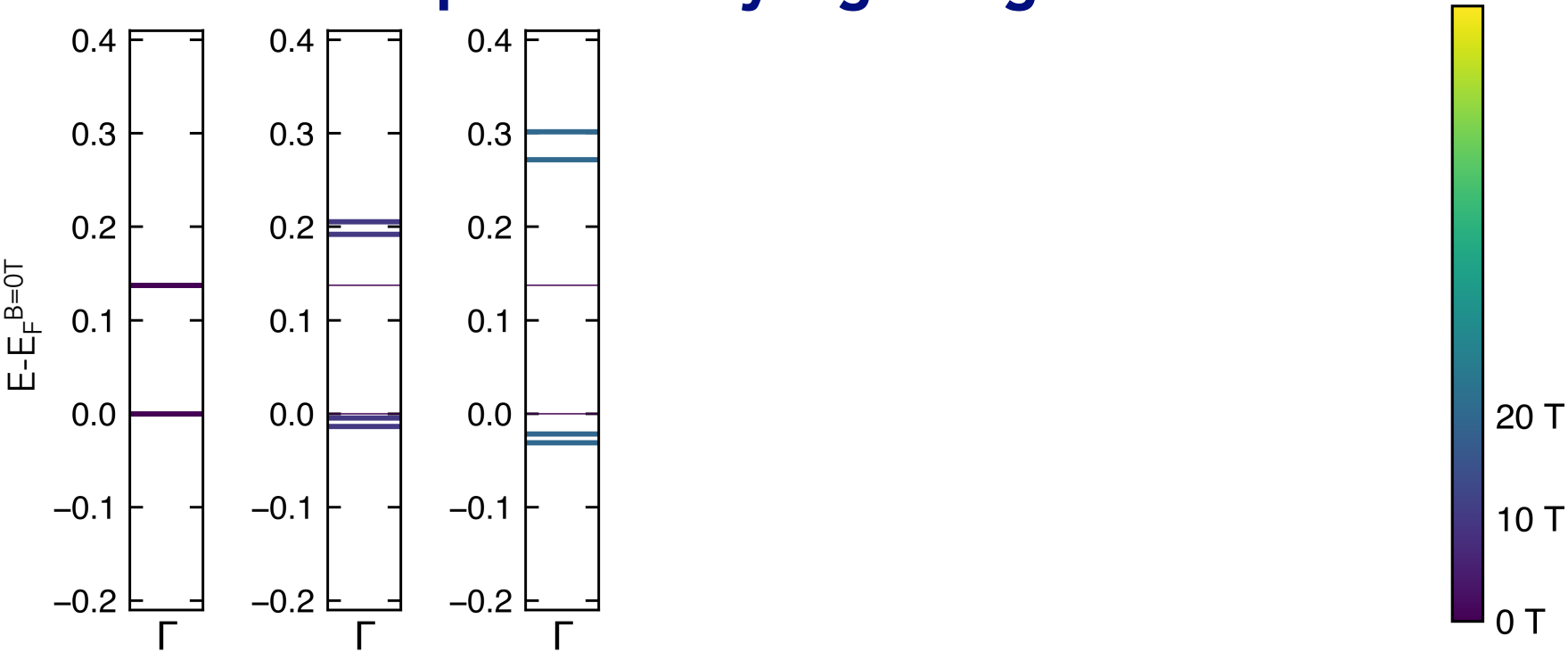

Peterson, Lane, Zhu, *in preparation*

Effects of experimentally high magnetic fields

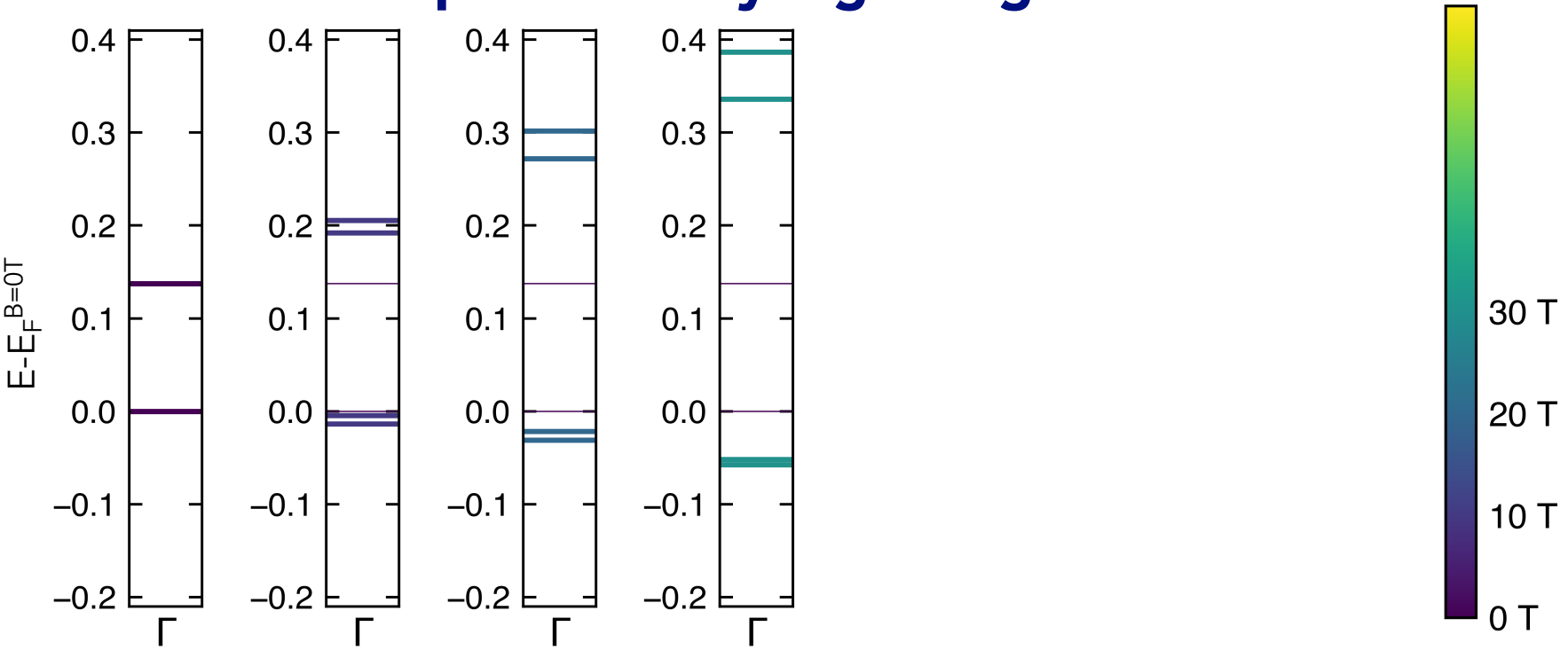

Peterson, Lane, Zhu, *in preparation*

Effects of experimentally high magnetic fields

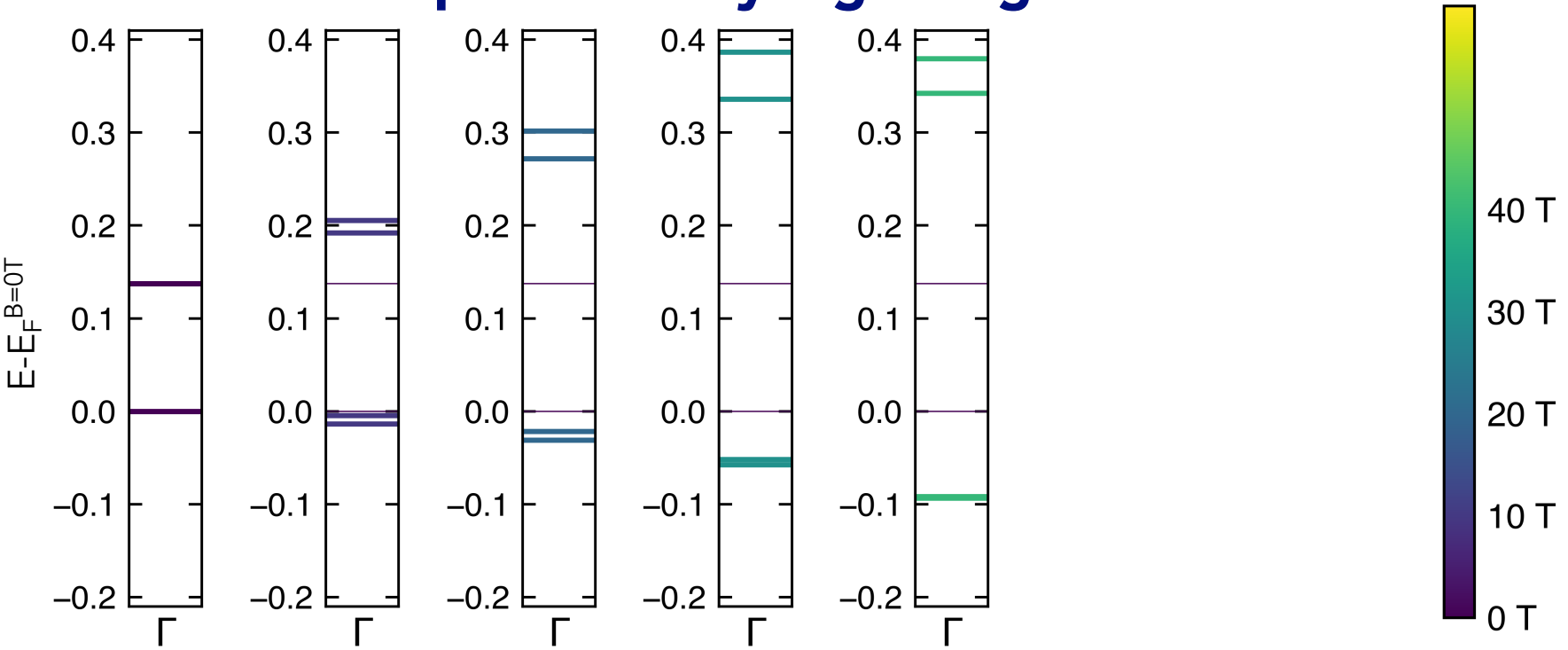

Peterson, Lane, Zhu, *in preparation*

Effects of experimentally high magnetic fields

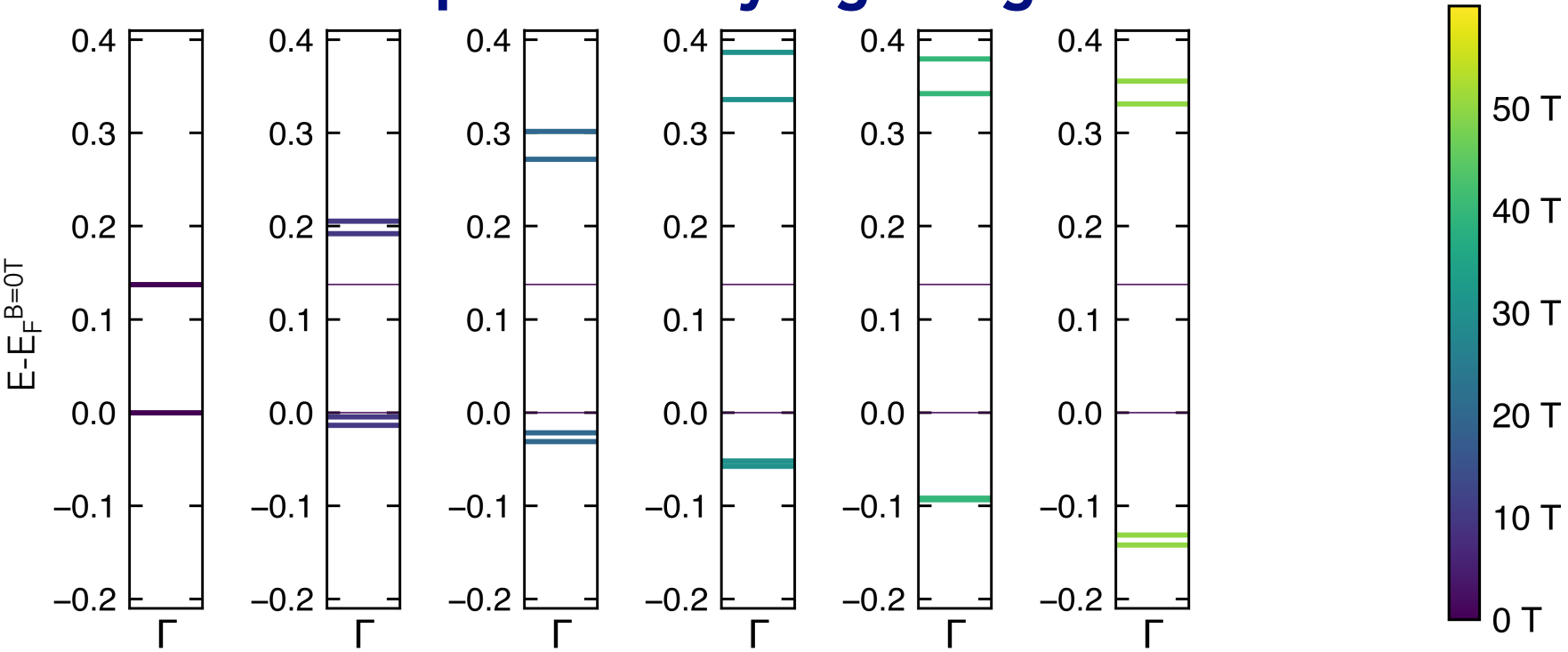

Peterson, Lane, Zhu, *in preparation*

Effects of experimentally high magnetic fields

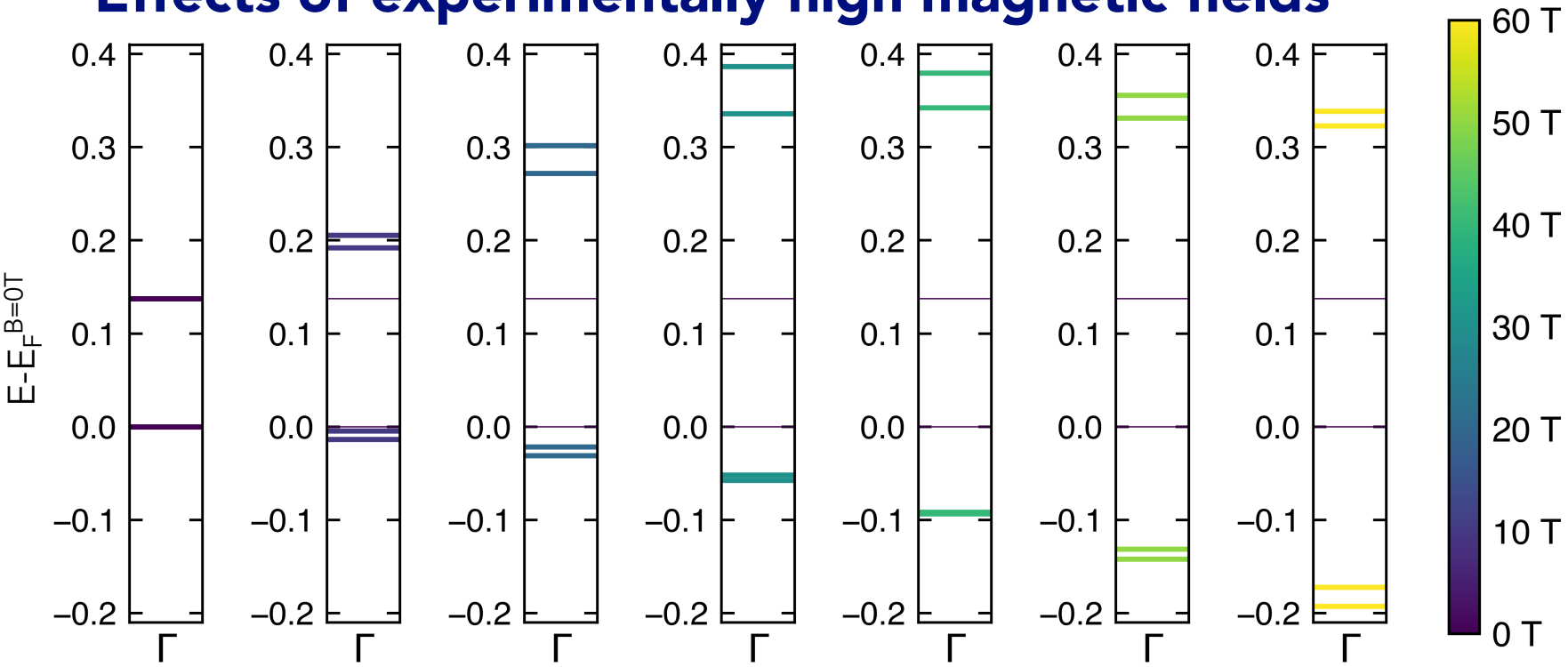

Applied magnetic field along chain direction

effective ***downward*** shift in chemical potential at **critical B field**

Peterson, Lane, Zhu, *in preparation*

Summary

Electronic structure calculations reveal that anomalous transport properties of $ZrTe_5$ and $HfTe_5$ arise from competition amongst various factors including:

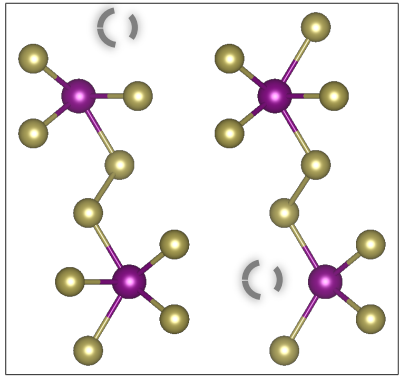

Te vacancies

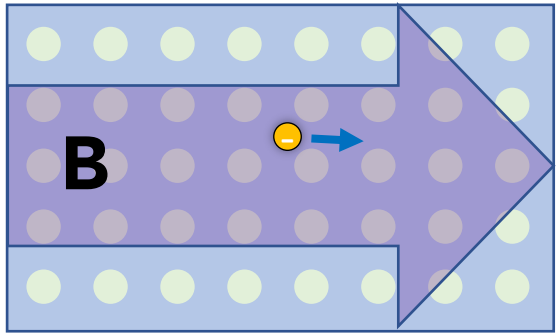

Applied B field

Next Steps

Calculation of **longitudinal and transverse conductivity,** compare to experiment

Acknowledgements

Collaborators

Jian-Xin Zhu

Christopher Lane

IMS Institute for Materials Science Los Alamos

Center for Integrated Nanotechnologies — DISCOVERY, PERFORMANCE, EDUCATION, INTEGRATION — CINT — Sandia, Los Alamos

NATIONAL HIGH MAGNETIC FIELD LABORATORY

Funding

LDRD LABORATORY DIRECTED RESEARCH & DEVELOPMENT

Back up Slides

Pristine band structures

No SOC

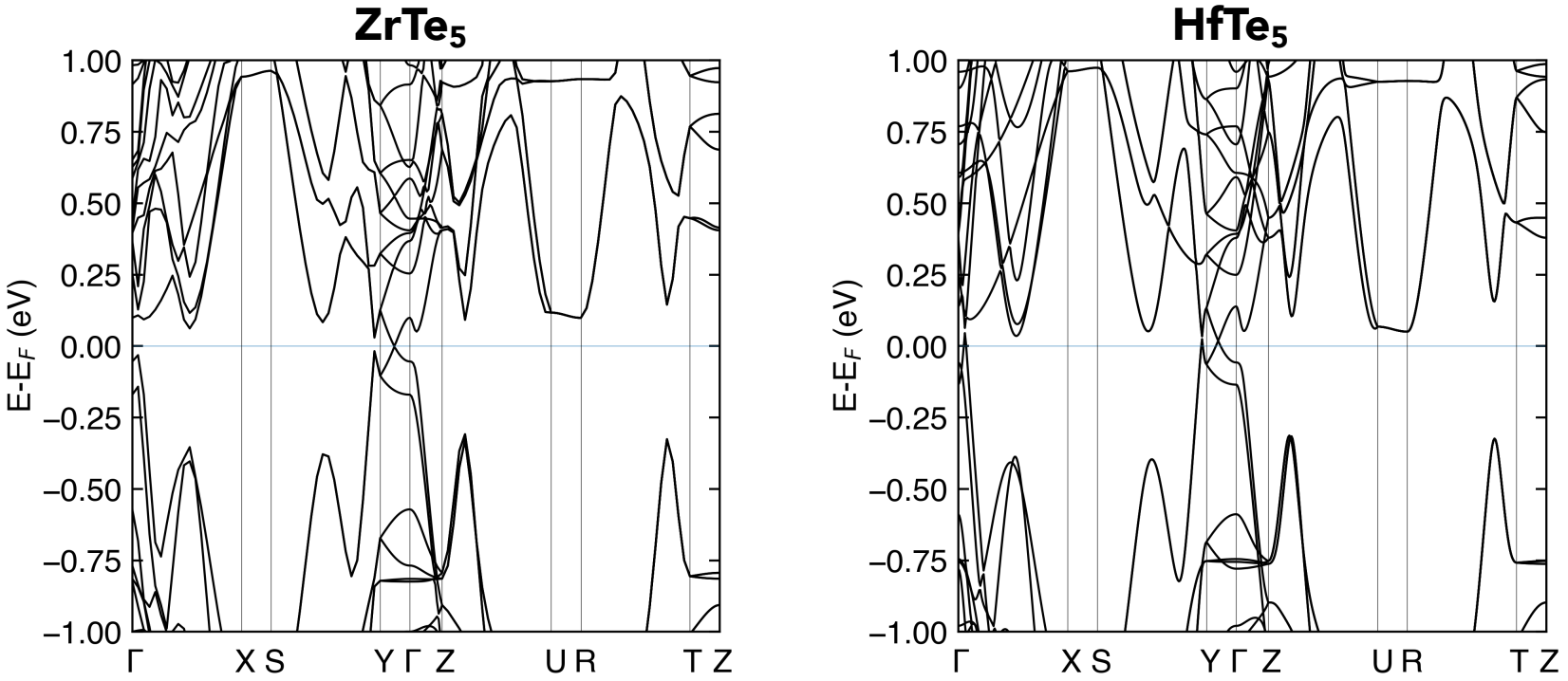

Pristine band structures

No SOC

SOC

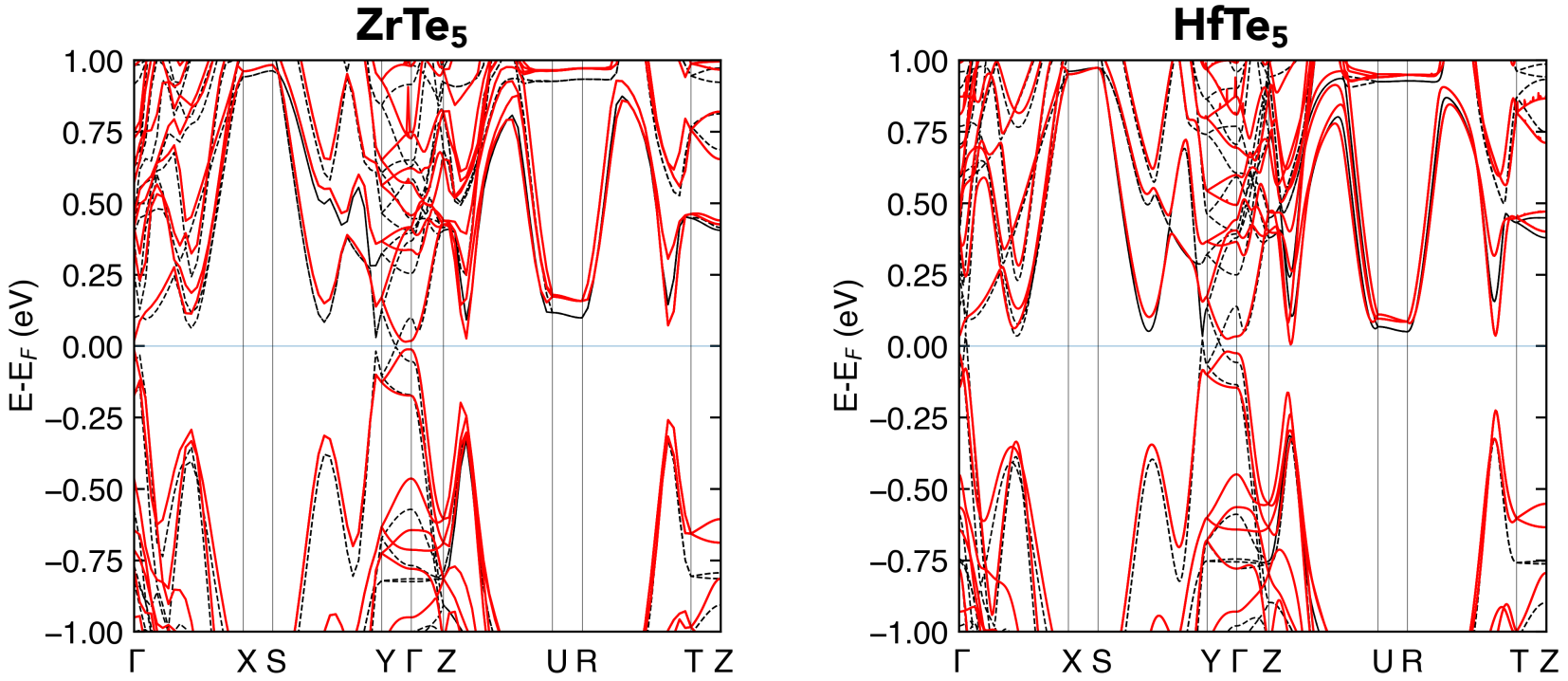

Spin-orbit coupling opens band gap

Is $ZrTe_5$ a Dirac semimetal?

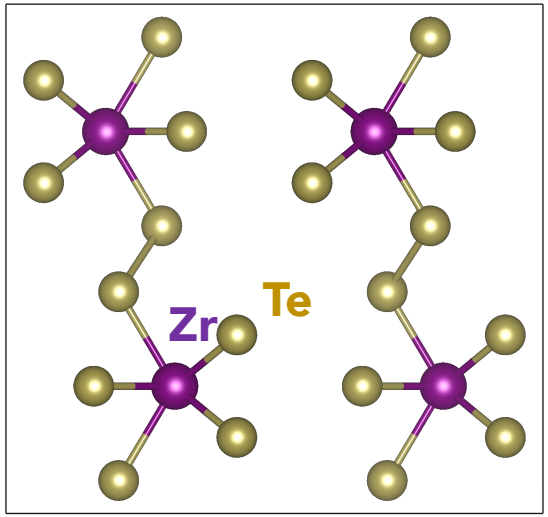

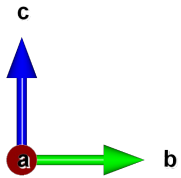

3D Dirac semimetal

SdH oscillations, ARPES, IR reflectivity

R. Y. Chen, et al., *PRL*, **115**, 176505 (2015)
R. Y. Chen, et al., *PRB*, **92**, 075107 (2015)
Q. Li, et al., *Nat. Phys.*, **12**, 550 (2016)
Y. W. Liu, et al., *Nat. Commun.*, **7**, 12516 (2016)
G. Zheng, et al., *PRB*, **93**, 115414 (2016)
W. Zhang, et al., *PRB*, **102**, 115147 (2020)

Weak Topological Insulator

STM, ARPES, First-principles

X. B. Li, et al., *PRL*, **116**, 176803 (2016)
R. Wu, et al., *PRX*, **6**, 021017 (2016)
L. Moreschini, et al., *PRB*, **94**, 081101 (2016)
Y. Zhang, et al., *Nat. Commun.*, **8**, 15512 (2017)

Strong Topological Insulator

First-principles

G. Manzoni, et al., *PRL*, **117**, 237601 (2016)

Strain induced change in electronic structure

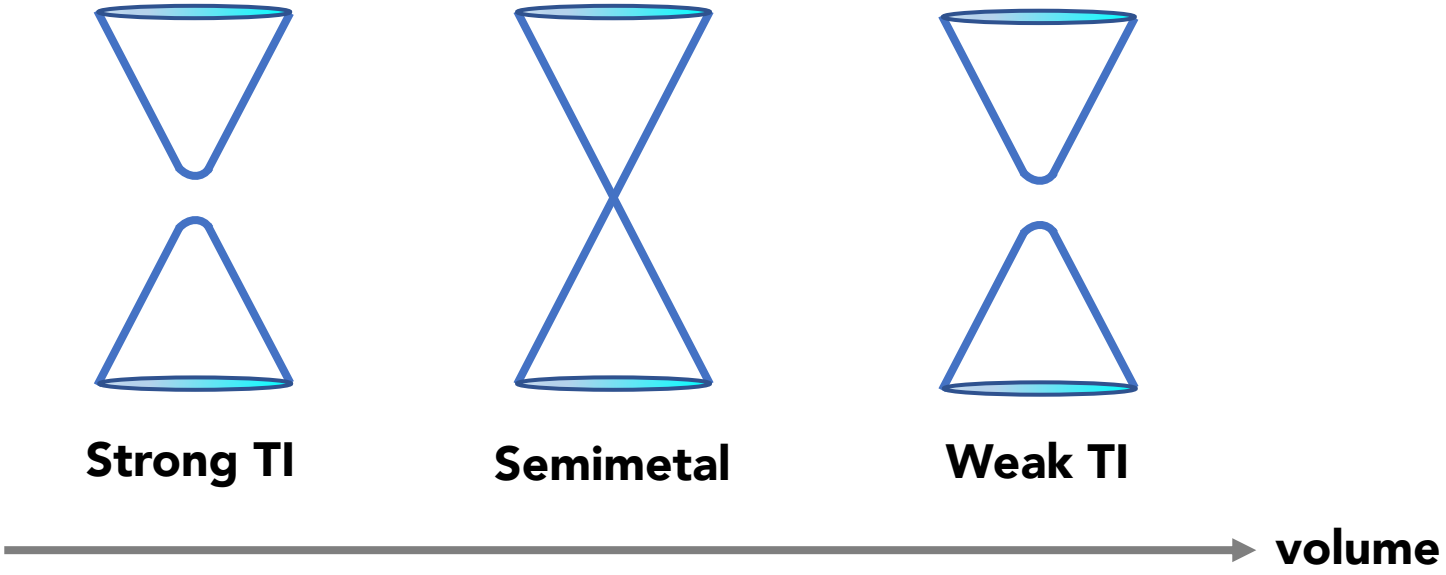

Band structure and topological indices of $ZrTe_5$ depends on volume/lattice parameters

Z. Fan, et al. *Sci Rep*, **7**, 45667 (2017)

Electrons interacting with electromagnetic fields

N Electrons in Electromagnetic Field (Semiclassical)

$$H = \frac{1}{2m}\sum_i \left(\boldsymbol{p}_i + \frac{e}{c}\boldsymbol{A}(\boldsymbol{r}_i)\right)^2 + \sum_i U_A(\boldsymbol{r}_i - \boldsymbol{R}_A) + \frac{1}{2}\sum_{i,j}\frac{e^2}{|\boldsymbol{r}_i - \boldsymbol{r}_j|} - \sum_i e\Phi(\boldsymbol{r}_i)$$

Vector potential

Ionic background

Electron-electron Coulomb potential

Scalar potential

Interaction Hamiltonian

$$H_{int} = \frac{e}{2mc}\sum_i [\boldsymbol{p}_i \cdot \boldsymbol{A}(\boldsymbol{r}_i) + \boldsymbol{A}(\boldsymbol{r}_i) \cdot \boldsymbol{p}_i] - e\sum_i \Phi(\boldsymbol{r}_i)$$

Dressel, Grüner, Electrodynamics of Solids, Cambridge University Press (2002)

Applied magnetic field

$$h_\alpha(\boldsymbol{r}) = \frac{\left[\frac{\hbar}{i}\nabla_{\boldsymbol{r}} + \frac{e}{c}\boldsymbol{A}(\boldsymbol{r})\right]^2}{2m_e} + V(\boldsymbol{r}) + \boldsymbol{S}_\alpha \cdot \boldsymbol{H}(\boldsymbol{r}) - E_F$$

Zeeman contribution

$H_Z \sim \boldsymbol{S} \cdot \boldsymbol{B}$

Really small!!!
B = 1T → ~50 μeV

Orbital contribution

Peierl's substitution

$$h_{ij}(\boldsymbol{r}) = -t_{i\neq j}e^{i\varphi_{ij}} + (\epsilon_i - E_F)\delta_{ij}$$

$$\varphi_{ij} = -\frac{e}{\hbar c}\int_{\boldsymbol{R}_j}^{\boldsymbol{R}_i} \boldsymbol{A}(\boldsymbol{\xi}) \cdot \boldsymbol{\xi}$$

Perturbative expansion of orbital contribution in A

Orbital contribution

$$h_{ij}(\boldsymbol{r}) = -t_{i\neq j}e^{i\varphi_{ij}} + (\epsilon_i - E_F)\delta_{ij}$$

$$\varphi_{ij} = -\frac{e}{\hbar c}\int_{\boldsymbol{R}_j}^{\boldsymbol{R}_i} \boldsymbol{A}(\boldsymbol{\xi})\cdot\boldsymbol{\xi}$$

$$\Rightarrow \quad h_{ij}(\boldsymbol{r}) = -t_{i\neq j}(1 + i\phi_{ij}) + (\epsilon_i - E_F)\delta_{ij}$$

Orbital contributions

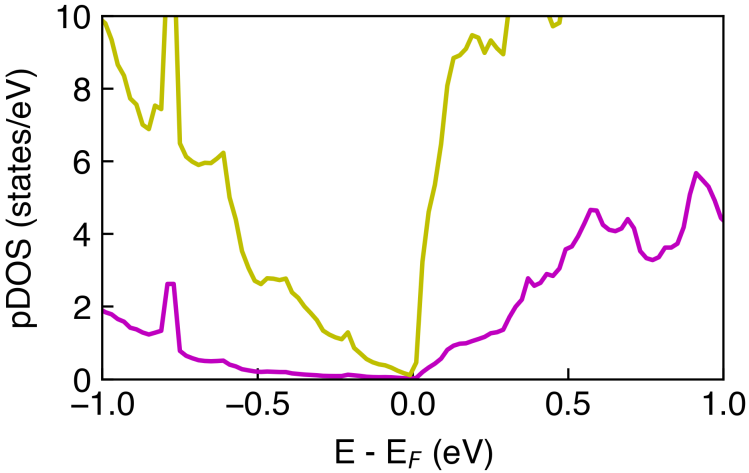

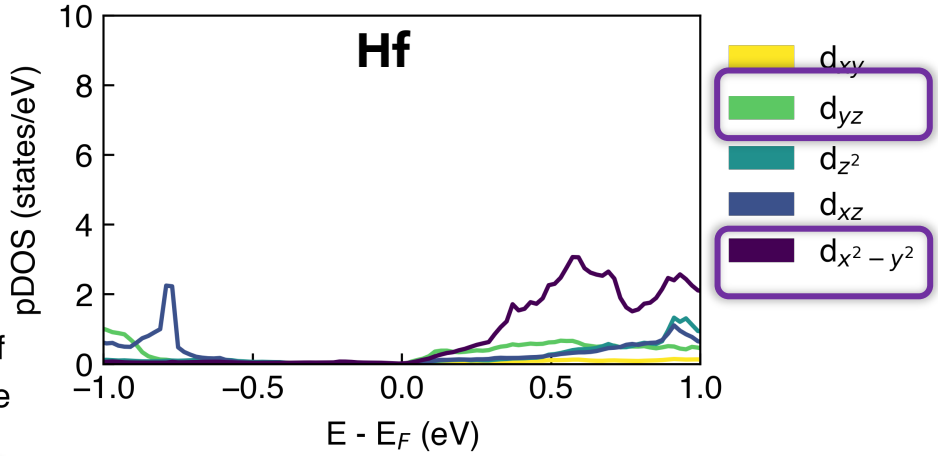

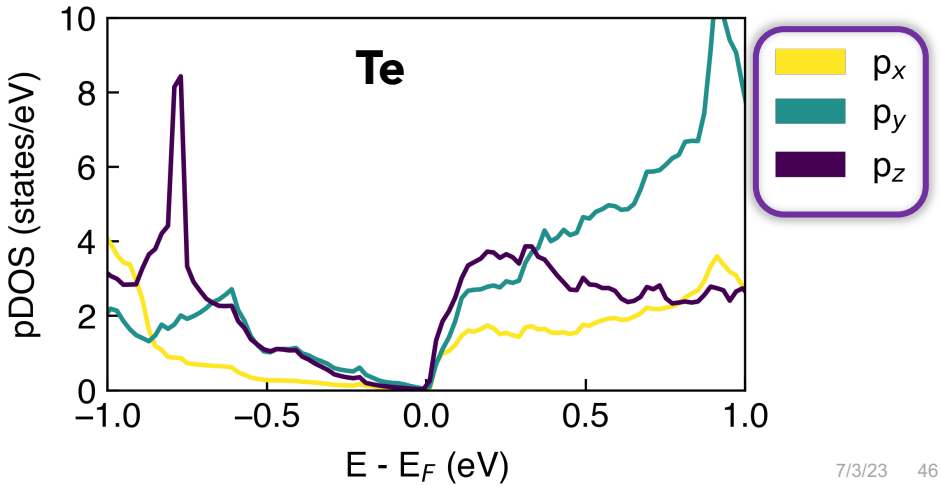

Orbitals near Fermi energy most important for transport

Wannierization

DFT codes for periodic systems produce wavefunctions in k-space

Bloch functions: $\psi_{n\boldsymbol{k}}(\boldsymbol{r}) = e^{i\boldsymbol{k}\cdot\boldsymbol{r}} u_{n\boldsymbol{k}}(\boldsymbol{r})$

$\boldsymbol{R}$: lattice vector $u_{n\boldsymbol{k}}(\boldsymbol{r}+\boldsymbol{R}) = u_{n\boldsymbol{k}}(\boldsymbol{r})$

$$u_{n\boldsymbol{k}}(\boldsymbol{r}) = \sum_{\boldsymbol{G}} c_{\boldsymbol{G}} e^{i\boldsymbol{G}\cdot\boldsymbol{r}}$$

$\boldsymbol{G}$: reciprocal lattice vector

Convert to "maximally localized" Wannier functions for real-space wavefunctions

$$w_{n\boldsymbol{R}}(\boldsymbol{r}) = \frac{V}{(2\pi)^3} \int_{BZ} \left[\sum_m U_{mn}^{(\boldsymbol{k})} \psi_{m\boldsymbol{k}}(\boldsymbol{r}) \right] e^{-i\boldsymbol{k}\cdot\boldsymbol{R}} d\boldsymbol{k}$$

Confirm selected Wannier functions reproduce DFT

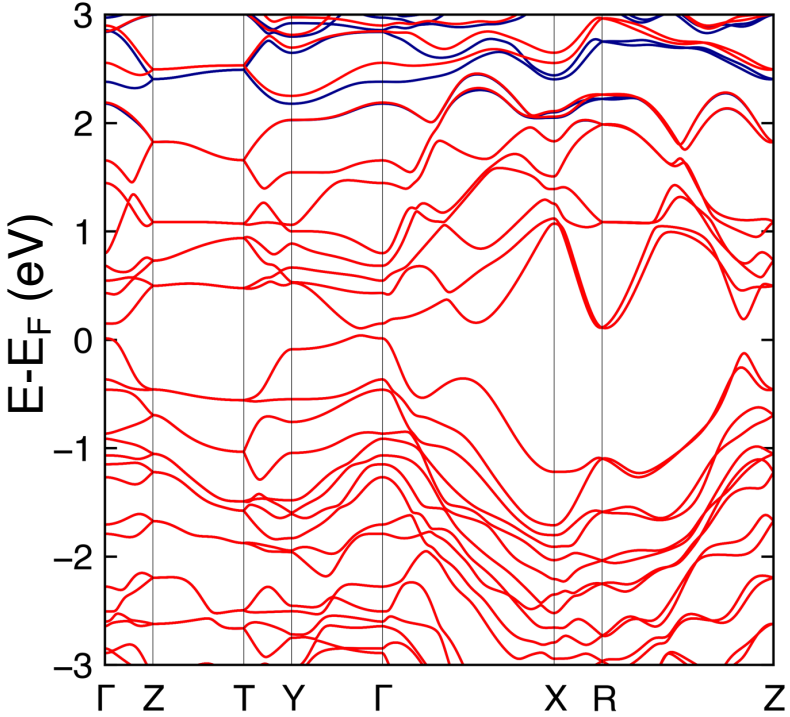

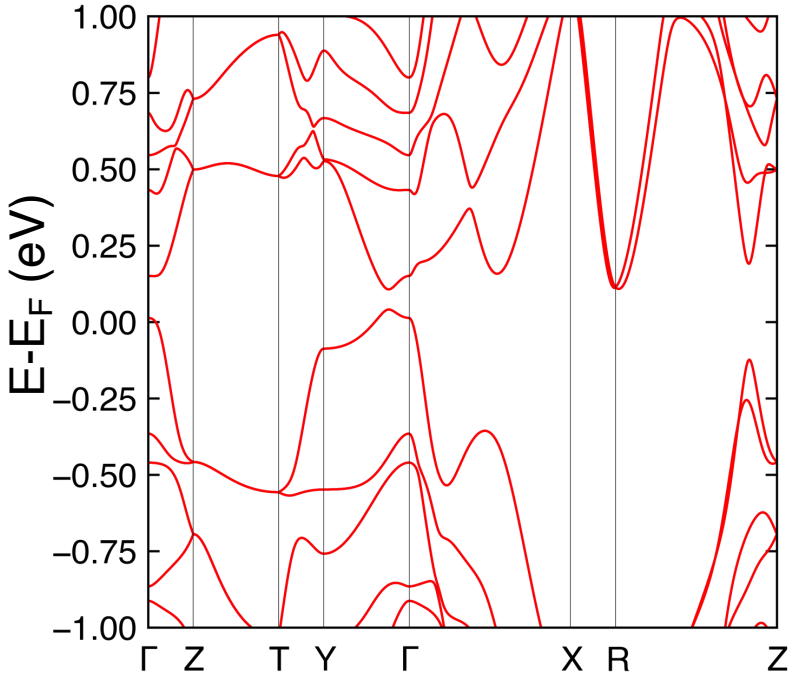

DFT Wannier function fit

Next Steps: Transport

Kubo Formula

$$\sigma_{\alpha\beta} = \sum_{nm\boldsymbol{k}} \frac{f(m\boldsymbol{k}+\boldsymbol{q}) - f(n\boldsymbol{k})}{(\varepsilon_{m\boldsymbol{k}+\boldsymbol{q}} - \varepsilon_{n\boldsymbol{k}})} \frac{< n\boldsymbol{k}|v_\alpha|m\boldsymbol{k}+\boldsymbol{q} >< m\boldsymbol{k}+\boldsymbol{q}|v_\beta|n\boldsymbol{k} >}{\varepsilon_{m\boldsymbol{k}+\boldsymbol{q}} - \varepsilon_{n\boldsymbol{k}} + i\delta}$$

Calculate **longitudinal and transverse conductivity** to compare to experiment